*Progress In Electromagnetics Research B, Vol. 31, 15–28, 2011*

# AN INVERSE PROBLEM APPROACH FOR PARAMETER ESTIMATION OF INTERIOR PERMANENT MAGNET SYNCHRONOUS MOTORS

**M. Hadef [1, 2, *], M. R. Mekideche [1], A. Djerdir [2], and A. Miraoui [2]**

[1]Université de Jijel, Laboratoire LAMEL, B.P. 98, Ouled Aissa 18000, Jijel-Algérie

[2]Electronic, Electrotechnical and Systems Laboratory, Technological University of Belfort-Montbéliard, France

**Abstract**—The estimation of $d$- and $q$-axis parameters is highly desirable, because they are fundamental parameters to many vector control algorithms in the $d$-$q$ reference frame for fast and accurate responses. Using the finite element method (FEM) for the determination of the interior permanent magnet synchronous motor (IPM) reactance provides an accurate means of determining the field distribution. However, this method might be time consuming. The magnetic circuit modelling approach has been successfully used to model a variety of electrical machine such as IPM motors. This paper deals with the inverse problem methodology for the identification of $d$- and $q$-axis synchronous reactance of an IPM motor. The proposed method uses a measured electromotive force (EMF) to compute the objective function. The machine parameters identified by the proposed approach are compared to experimental results.

## 1. INTRODUCTION

The interior permanent magnet synchronous motors (IPMSM) are widely used in automotive and other servo drives due to their superior advantages and positive features, such as high efficiency, high torque density, high power factor, high power density, and wide speed range operation. However, the precise knowledge of parameters is of critical importance for correct performance prediction and design optimization of permanent magnet motors [1–3]. The reactance parameters of

*Received 12 February 2011, Accepted 23 May 2011, Scheduled 29 May 2011*

* Corresponding author: Mounir Hadef (hadef_mounir@yahoo.fr).

PMSM are most essential to the performance analysis and optimization design of the motor [4–7]. As for the PMSM speed adjustment, the exact calculated reactance parameters is a key issue for implementing the control algorithm and predicting the steady state and transient characteristics of PMSM [2].

A great deal of techniques have been developed for estimating the synchronous machine parameters and determining their characteristics. Some of them are based on standstill tests, while others are based on frequency tests [5, 8, 9]. However, for PMSM there are no open and short circuit states unlike electrical excited motors, since the excitation of permanent magnet materials is affected at all the time. With a different magnetic force and field saturation the reactance and the inductance parameters are also different [1, 3, 4, 10]. Thus, any parameter estimation method should also consider the influence of the PM motor.

However, while numerical techniques, like finite-element analysis provide an accurate means of determining the field distributions taking into account the saturation [3, 8, 9] they are somewhat time-consuming and do not provide as much insight as analytical solutions into the influence of the design parameters on the machine behaviour.

The magnetic equivalent circuit (MEC) modelling approach has been successfully used to model a variety of electrical machines, such as interior permanent magnet synchronous motor by using information on torque, flux, magnetic motive force (MMF), and electromotive force (EMF) [1, 9, 11]. The improved MEC is different from the finite element method (FEM) in two aspects. Firstly, the number of elements developed for the MEC method is much less than that required by the FEM. Secondly, in the MEC, the flux can pass through an element only in the specified direction, whereas in the FEM there is no restriction on the direction of flux trough any element.

Inverse problem, arise in several domains of science and technology like medical imaging, electromagnetic scattering, system identification [12–15]. The main difficulty in taking inverse problems is due to its intrinsic ill-posed nature [14, 15] where arbitrarily small changes in data may lead up to arbitrarily large changes in the solution. The parameter identification inverse problem is of important practical problem in many science fields and is usually treated as an optimization problem, where the objective function to be examined gives the mismatch between the measured values and the simulated results in a Euclidean norm (least-squares method) or in any other appropriate norm [14, 16, 17]. Like in numerical treatment of inverse problems, data errors are inevitable, and the so-called regularization methods are to be used for stabilizing procedures for successfully dealing with ill-posed problems. Actually, the effectiveness of a regularization method depends strongly on the choice of a good regularization parameter [15]. However, a trial-and-error approach is used to find a reasonably good parameter. In this paper, an identification approach based on inverse problem methodology is proposed and applied to a laboratory interior permanent magnet synchronous motor used in [10]. The magnetic circuit model of the IPM motor is used as the direct model. In order to estimate the $d$- and $q$-axis synchronous reactance, the open circuit EMF is used to compute the objective function. The simulation results compared to laboratory tests of [10] verify the proposed method.

## 2. MAGNETIC CIRCUIT MODEL OF IPM MOTOR

In order to assess the validity of the inverse problem parameter estimation, an IPM motor with tangential magnet poles is considered in this paper. Fig. 1 shows a one pole pitch cross sectional view of a 6-pole IPM motor. In this configuration the buried magnets are magnetized along their shorter dimensions along the $d$-axis. For simplicity it is assumed that there is no magnetic saturation in either the stator or the rotor steel [10]. The equivalent magnetic circuit is shown in Fig. 2. By definition, $\phi_g/2$ is the air gap flux through one half of the air-gap cross sectional area, $\phi_r/2$ is the flux source of the one half of the magnet. $2R_g$ is the reluctance of one-half of the air gap with compensation for slotting, $2R_{m0}$ is the reluctance of one half of a magnet, $R_{m1}$ is the

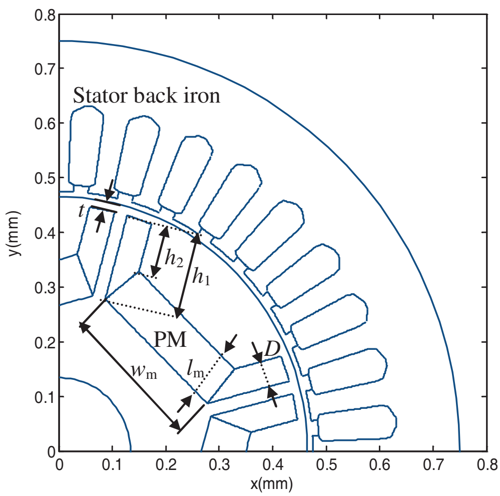


**Figure 1.** IPM synchronous motor structure.

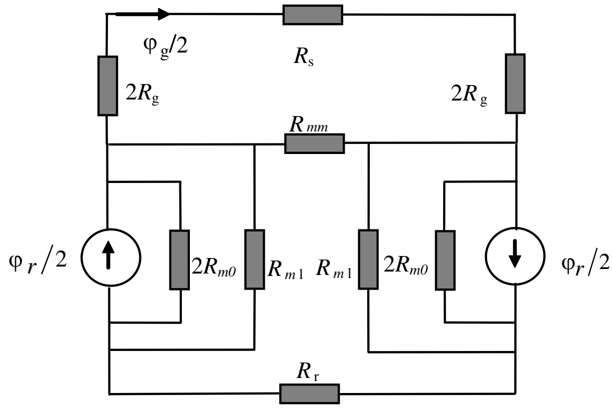


**Figure 2.** Magnetic circuit model of IPM synchronous motor.

reluctance modelling the flux linkage.

The value of these reluctance can be calculated by applying Ampere's law as shown beneath

$$R_g = \frac{K_c g}{\mu_0 A_g} \tag{1}$$

$$R_{m0} = \frac{l_m}{\mu_0 \mu_{rec} A_m} \tag{2}$$

$$R_{m1} = \frac{4d}{\mu_0 l (h_1 + h_2)} \tag{3}$$

where $A_g$ and $A_m$ are the cross-sectional areas per pole of the air gap and magnet respectively, $K_c$ is the cater coefficient, $g$, $l_m$ and $l$ are the air gap length, the magnet length in the direction of magnetization and the stack length respectively. $d$, $h_1$ and $h_2$ are width of the flux barrier, and the heights, $\mu_0$ and $\mu_{rec}$ are the permeability of the free space and the relative recoil permeability of the magnet.

$R_r$ and $R_s$ are the reluctance of the rotor and stator back irons. These reluctance are ignored here under the assumption of no saturation.

The air gap flux $\phi_g$ is related to the remnant flux $\phi_r$ by

$$\phi_g = \frac{1}{1 + \beta(1 + 2\eta + 4\lambda)} \phi_r \tag{4}$$

where $\beta = R_g/R_{m0}$ is the reluctance ratio. $\eta = R_{m0}/R_{m1}$ and $\lambda = R_{m0}/R_{mm}$ are the leakage flux ratios.

The leakage flux consists of two components

$$\phi_{mt} = \phi_{mm} + \phi_{ml} \tag{5}$$

$\phi_{mm}$ is the flux leakage of the bridge between pole pieces given by

$$\phi_{mm} = \frac{2\beta\lambda}{1 + \beta(1 + 2\eta + 4\lambda)}\phi_r \tag{6}$$

$\phi_{ml}$ is the leakage flux flowing in a circular direction through the air flux barriers under the bridge given by

$$\phi_{ml} = \frac{\beta\eta}{1 + \beta(1 + 2\eta + 4\lambda)}\phi_r \tag{7}$$

By summing the air gap and the total leakage flux the magnet flux is given by

$$\phi_m = \frac{1 + \beta(2\eta + 4\lambda)}{1 + \beta(1 + 2\eta + 4\lambda)}\phi_r \tag{8}$$

Thus, the average air gap flux density and the corresponding magnet flux density are determined as

$$B_g = \frac{C_\phi}{1 + \beta(1 + 2\eta + 4\lambda)}B_r \tag{9}$$

$$B_m = \frac{1 + \beta(2\eta + 4\lambda)}{1 + \beta(1 + 2\eta + 4\lambda)}B_r \tag{10}$$

where $C_\phi = A_m/A_g$ is the flux concentration factor, $B_r$ is the remnant magnetization.

The amplitude of the fundamental component of the air gap flux due to the magnet acting alone is

$$B_{M1} = \frac{4}{\pi}B_g \sin\left(\frac{\alpha\pi}{2}\right) \tag{11}$$

where $\alpha$ is the pole arc to pole-pitch ratio.

The fundamental open-circuit flux per pole can be determined as

$$\phi_{M1} = \frac{Dl}{p}B_{M1} \tag{12}$$

where $D$ is the stator bore diameter, $l$ is stack length and $p$ is the number of pole pairs.

The $d$- and $q$-axis synchronous reactance can be given as

$$X_d = \frac{6\mu_0 Dlf}{p^2 g''_d}(K_{W1}N_{ph})^2 + X_\sigma \tag{13}$$

$$X_q = \frac{6\mu_0 Dlf}{p^2 g''_q}(K_{W1}N_{ph})^2 + X_\sigma \tag{14}$$

where $\mu_0$ is the permeability of the free space, $f$ the frequency, $K_{W1}$ and $N_{ph}$ are the fundamental harmonic winding factor and the number of series turns per phase respectively, and $X_\sigma$ is the armature leakage reactance given by Eq. (A1) in Appendix.

$g''_d$ is the effective air gap length in the direct-axis allowing for the magnet and $g''_q$ is the effective air gap length in the quadrature axis respectively, they are given by

$$g''_d = \frac{K_c g}{K_{1ad} - (K_1 K_{\alpha d}/1 + \beta(1 + 2\eta + 4\lambda))} \tag{15}$$

$$g''_q = \frac{K_c g}{K_{1aq}} \tag{16}$$

$K_1$, $K_{1ad}$, $K_{1aq}$ and $K_{\alpha d}$ are given in the appendix.

For a practical winding with $N_{ph}$ series turns per phase and a winding factor $K_{W1}$, the open-circuit EMF per phase can be determined as

$$E_q = \frac{2\pi}{\sqrt{2}} K_{W1} N_{ph} \phi_{M1} f \tag{17}$$

## 3. INVERSE PROBLEM PARAMETER ESTIMATION

Parameter estimation is commonly accepted as a fundamental step for the system identification process. The concept includes systems where it may not be possible to write mathematical equations that accurately describe the processes of interest. In general, in a system identification problem or an inverse problem, the fundamental properties are to be determined from the observed behaviour of the system [15, 16]. The objective of this study is to investigate and develop a system identification model based on the inverse problem theory, to determine the permanent magnet synchronous motor parameters such as the $d$- and $q$-axis synchronous reactance. The knowledge of the flux linkage is enough for the complete characterization of the machine and can be used for the machine control development.

### 3.1. Problem Formulation

Permanent magnet synchronous motors can be treated uniformly within the framework of the widely used two-axis theory. The analysis of a PM motor is usually based upon the constant parameters of the two-axis model of the motor. In general these parameters are not constant, but vary in dependence of load conditions and the level saturation flux paths in the motor [3, 5]. Setting $X_1 = X_d$, $X_2 = X_q$, $X_3 = \phi_{M1}$ and substituting $K_{W1} N_{ph}$ from Eq. (13) and Eq. (14) into Eq. (17) yields

$$E_q(X_1, X_2, X_3) = \frac{\pi}{\sqrt{3t_1}} p f X_3 \sqrt{X_1 - X_2} \tag{18}$$

where $t_1$ is a constant given by

$$t_1 = \mu_0 D f l \left( \frac{1}{g_d''} - \frac{1}{g_q''} \right) \tag{19}$$

The parameter identification is typically defined for identifying the continuous vector $X$, given a set of continuous experimental data $U$. To solve it, a parameter identification problem is often converted to the minimization of a continuous problem

$$\mathrm{Min}\, f(X) \tag{20}$$

where $f$ is the reconstruction error or the objective function to be minimized.

The inverse problem can be therefore formulated as follows

$$\text{Minimize} \quad F(X) = \left( \frac{E_q^C}{E_0} - 1 \right)^2 \tag{21}$$

$$\begin{array}{ll} \text{Subject to} & E_q(X_1, X_2, X_3) = \frac{\pi}{\sqrt{3t_1}} p f X_3 \sqrt{X_1 - X_2} \\ & 0.21 \leq X_1 \leq 0.30 \\ & 0.45 \leq X_2 \leq 0.60 \\ & 0.0008 \leq X_3 \leq 0.0020 \end{array} \tag{22}$$

where $E_q^C$ and $E_0$ are the computed and the measured open-circuit EMF per phase, and $X = [X_d \quad X_q \quad \phi_{M1}]$ is the vector parameter.

## 3.2. Regularization

The concept of well-posed and ill-posed problems goes back to Hadamard who essentially defined a problem to be ill-posed if the solution is not unique or if it is not a continuous function of the data [18]. Hence, it is necessary to incorporate further information about the desired solution in order to stabilize the problem and to single out a useful and stable solution. This is the purpose of regularization, and the Tikhonov's regularization technique is an effective tool for ill-posed problems solution and the analysis of ill-conditioned linear systems [14, 15]. The Tikhonov regularization method introduces a regularization term $F_r$ representing roughly, the least-squared difference between the initial guessed $X^0$ and the current calculated one.

$$F^* = (1 - \lambda) F + \lambda F_r \tag{23}$$

where $\lambda > 0$, is the regularization parameter.

The Tikhonov regularization term is given by

$$F_r = \sum_i \left( X_i^k - X_i^0 \right)^2 \tag{24}$$

where $X_i^0$ and $X_i^k$ are the initial and the current set of parameters respectively.

The optimal choice of the regularization parameter realizes the perfect trade-off between the complexity of the solution and its ability to reliably reproduce the experimental data. Several numerical methods have been proposed to choose the optimal regularization parameter for Tikhonov regularization such as the L-curve method [15, 19].

## 4. RESULTS AND DISCUSSION

In order to assess the proposed estimation parameter method based on inverse problem theory, numerical analysis was performed on IPM motor.

Table 1 shows the main specifications of the IPM motor. The inverse algorithm is implemented by using "Fmincon" from MATLAB®'s OPTIMIZATION TOOLBOX: this local solver finds a local minimum of a constrained multivariable function by means of sequential quadratic programming (SQP) algorithm. The method uses numerical or, if available analytical gradients. In the cases under study the gradients are calculated analytically. An Fmincon iteration

**Table 1.** Specifications of the IPM motor.

| Parameters | Symbols | Values |
|---|---|---|
| Stator bore radius | $r_1$ | 47.5 mm |
| Air gap length | $g$ | 1.00 mm |
| Bridge width | $t$ | 1.5 mm |
| Flux barrier width | $D$ | 4.00 mm |
| Flux barrier height | $h_1$ | 15.904 mm |
| Flux barrier height | $h_2$ | 8.885 mm |
| Magnet width | $W_m$ | 27.7 mm |
| Magnet thickness | $l_m$ | 8.10 mm |
| Ramanent flux density | $B_r$ | 1.05 T |
| Saturation flux density | $B_s$ | 1.88 T |
| Recoil permeability | $\mu_{rec}$ | 1.05 |
| Pole pairs | $p$ | 3 |
| Frequency | $f$ | 360 Hz |
| Rated current | $I$ | 19 A |
| Series turns per phase | $N_{ph}$ | 30 |
| Winding factor | $K_{w1}$ | 0.644 |

consists of three main stages: updating of the Hessian matrix of the Lagrangian function, quadratic programming problem solution, and line search and merit function. Since the SQP method is very effective when starting from an initial points close to the feasible region, the optimization process was started from a reasonable initial guess $X^{(0)} = [0.24 \quad 0.53 \quad 0.001]$ where the objective function is $F^{(0)} = 0.00209386$. In many cases the optimal regularization parameter from Tikhonov regularization is determined by the L-curve method, which is a plot of the solution norm versus the corresponding residual norm for all valid regularization.

In literature it is shown by numerical examples that typical suitable value, of $\lambda$ are in the range of $\lambda < 1$. As seen from Table 2, $\lambda$ was varied manually in order to asses its influence on the reconstructed results. The inverse design converged after 7 iterations to satisfy the stopping criterion by which the function value changes are less than the specified tolerance. The optimal deign is $X^{(7)} = [0.246 \quad 0.528 \quad 0.0015]$ for a parameter regularization $\lambda = 10^{-12}$. Table 3 displays the objective function versus the iterations. The parameter estimation results obtained with the analytical model and inverse problem model are presented in Table 4.

Comparing the obtained results via the inverse problem approach

**Table 2.** Optimization process.

| $\lambda$ | Iteration | $X_d\,(\Omega)$ | $X_q\,(\Omega)$ | $\phi_{M1}\,(Wb)$ | Objective Function |
|---|---|---|---|---|---|
| $10^{-1}$ | 8 | 0.2459 | 0.5301 | 0.0015 | $1.35675e-9$ |
| $10^{-2}$ | 8 | 0.2453 | 0.5301 | 0.0015 | $5.03268e-9$ |
| $10^{-3}$ | 8 | 0.2452 | 0.5301 | 0.0015 | $1.08008e-9$ |
| $10^{-4}$ | 7 | 0.2460 | 0.5280 | 0.0015 | $4.31063e-10$ |
| $10^{-5}$ | 7 | 0.2460 | 0.5280 | 0.0015 | $6.41672e-11$ |
| $10^{-6}$ | 7 | 0.2460 | 0.5280 | 0.0015 | $2.67069e-11$ |
| $10^{-7}$ | 7 | 0.2460 | 0.5280 | 0.0015 | $2.29531e-11$ |
| $10^{-8}$ | 7 | 0.2460 | 0.5280 | 0.0015 | $2.25775e-11$ |
| $10^{-9}$ | 7 | 0.2460 | 0.5280 | 0.0015 | $2.25400e-11$ |
| $10^{-10}$ | 7 | 0.2460 | 0.5280 | 0.0015 | $2.25363e-11$ |
| $10^{-11}$ | 7 | 0.2460 | 0.5280 | 0.0015 | $2.25359e-11$ |
| $10^{-12}$ | 7 | 0.2460 | 0.5280 | 0.0015 | $2.25358e-11$ |
| $10^{-13}$ | 7 | 0.2460 | 0.5280 | 0.0015 | $2.25358e-11$ |
| $10^{-14}$ | 7 | 0.2460 | 0.5280 | 0.0015 | $2.25359e-11$ |
| $10^{-15}$ | 7 | 0.2460 | 0.5280 | 0.0015 | $2.25359e-11$ |
| $10^{-16}$ | 7 | 0.2460 | 0.5280 | 0.0015 | $2.25359e-11$ |
| $10^{-17}$ | 7 | 0.2460 | 0.5280 | 0.0015 | $2.25359e-11$ |

**Table 3.** Evolution of the objective function versus iterations.

| Iteration | Objective Function |
|---|---|
| 0 | 0.00209386 |
| 1 | $6.48234e-5$ |
| 2 | $5.59311e-5$ |
| 3 | $3.19436e-5$ |
| 4 | $3.51569e-9$ |
| 5 | $1.49117e-10$ |
| 6 | $1.49023e-10$ |
| 7 | $2.25358e-11$ |

**Table 4.** Comparison of parameter estimation results.

| Parameter | Analytical model | Error (%) | Inverse problem model | Error (%) | Test [10] |
|---|---|---|---|---|---|
| $X_d(\Omega)$ | 0.2684 | 2.24 | 0.2460 | 0 | 0.246 |
| $X_q(\Omega)$ | 0.5460 | 1.1 | 0.5280 | 0.7 | 0.535 |
| $\phi_{M1}(Wb)$ | 0.0015 | / | 0.0015 | / | / |

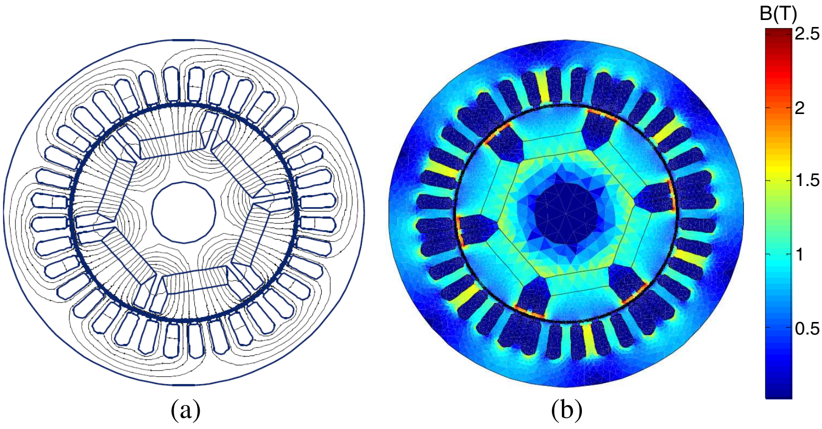


**Figure 3.** Flux density in the motor in typical operating conditions. (a) Equipotential lines. (b) Flux density map.

to those of test [10], Table 4 clearly shows the superiority in terms of solution quality of the proposed inverse method. A 2D FEM analysis is carried out by using the MATLAB®'s PDE TOOLBOX software to evaluate the results for a case study motor in typical operating

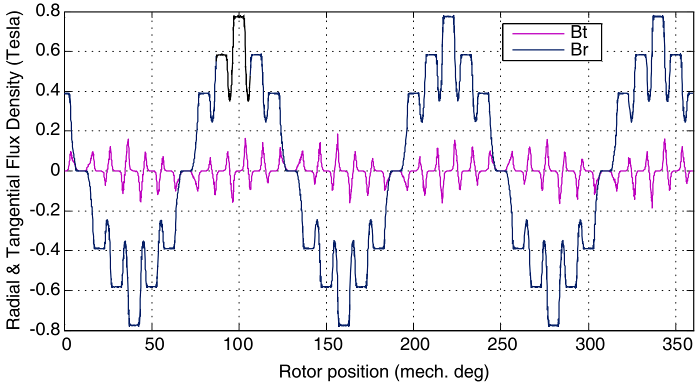


**Figure 4.** Radial and tangential component waveforms of the air-gap flux density.

conditions.

Figure 3(a) shows the distribution of the equipotential lines while Fig. 3(b) shows the distribution of the flux density in a PM motor. The radial and tangential component waveforms of the air-gap flux density with rotor position are shown in Fig. 4.

## 5. CONCLUSION

The method presented in this paper works very well in estimating the machine parameters of an interior permanent magnet synchronous motor. Based on the magnetic circuit as the direct model, the results indicate that the proposed approach was successfully used to estimates the $d$- and $q$-axis synchronous reactance and the open-circuit flux. It has the potential for high accuracy and robustness to measurements data using for computational cost.

## APPENDIX A.

The leakage reactance $X_\sigma$ of the armature windings of a.c. machines consists of the slot, the end-connection differential and tooth-top leakage reactance given by [20]

$$X_\sigma = 4\pi\mu_0 f \frac{N_{ph}^2 L_i}{pq_1}\left[\lambda_{\sigma s} + \frac{l_{1e}}{L_i}\lambda_{\sigma e} + \lambda_{\sigma d} + \lambda_{\sigma t}\right] \tag{A1}$$

where $q_1$ is the number of slot per pole per phase, $l_{1e}$ is the length of a single end connection, $X_{\sigma s}$, $X_{\sigma e}$, $X_{\sigma d}$ and $X_{\sigma t}$ are the slot, end connection differential and tooth-top leakage permeance.

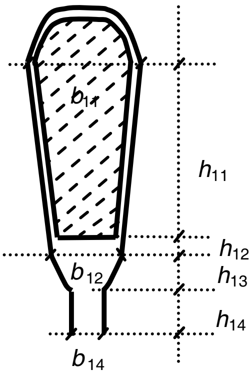


**Figure A1.** Semi-closed oval slot.

For a semi-closed oval slot as shown in Fig. A1, the specific slot leakage permeance is given by

$$\lambda_{\sigma s} = 0.1424+\frac{h_{11}}{3b_{12}}k_t+\frac{h_{12}}{b_{12}}+0.5\arcsin\left(\sqrt{1-(b_{14}/b_{12})^2}\right)+\frac{h_{14}}{b_{14}} \quad \text{(A2)}$$

where

$$k_t = \frac{3(4t^2-t^4(3-4\ln t)-1)}{4(t^2-1)^2(t-1)}, \quad t=\frac{b_{11}}{b_{12}} \quad \text{(A3)}$$

The end connection leakage permeance for almost all windings is given as

$$\lambda_{\sigma e} \approx 0.3q_1 \quad \text{(A4)}$$

The specific permeance of the differential leakage flux is

$$\lambda_{\sigma d} = \frac{3q_1 D_{1in} K_{w1}^2 \tau_{d1}}{2\pi\, pg K_c K_{sat}} \quad \text{(A5)}$$

where $\tau_{d1}$ is the differential leakage factor, $D_{1in}$ is the inner diameter of the stator, $K_C$ and $K_{sat}$ are the Carter's coefficient and the saturation factor respectively.

The tooth-top specific permeance is given by

$$\lambda_{\sigma t} \approx \frac{5g/b_{14}}{5+4g/b_{14}} \quad \text{(A6)}$$

$K_1$, $K_{1ad}$, $K_{1aq}$ and $K_{\alpha d}$ constants of Eq. (15) and Eq. (16) are given by

$$K_1 = (4/\pi)\sin(\alpha\pi/2) \quad \text{(A7)}$$
$$K_{1ad} = \alpha+(\sin\alpha\pi)/\pi \quad \text{(A8)}$$
$$K_{1aq} = \alpha+\Omega+(\sin\Omega\pi-\sin\alpha\pi)/\pi \quad \text{(A9)}$$
$$K_{\alpha d} = \sin(\alpha\pi/2)/(\alpha\pi/2) \quad \text{(A10)}$$

## REFERENCES

1. Lovelace, E. C., T. M. Jahns, and J. H. Lang, "A saturating lumped-parameter model for an interior PM synchronous machine," *IEEE Trans. on Industry Applications*, Vol. 38, No. 3, 645–650, May–Jun. 2002.
2. Bernal, F. F., A. G. Cerrada, and R. Faure, "Determination of parameters in interior permanent-magnet synchronous motors with iron losses without torque measurement," *IEEE Trans. on Industry Applications*, Vol. 37, No. 5, 1265–1272, Sep.–Oct. 2001.
3. Rezaie, J., M. Gholami, R. Firouzi, T. Alizadeh, and K. Salashoor, "Interior permanent magnet synchronous motor (IPMSM) adaptive genetic parameter estimation," *Proceedings of the WCECS*, Oct. 2007.
4. Meessen, K. J., P. Thelin, J. Soulard, and E. A. Lomonova, "Inductance calculations of permanent-magnet synchronous machines including flux change and self- and cross-saturations," *IEEE Trans. on Magnetics*, Vol. 44, No. 10, 2324–2331, Oct. 2008.
5. Gieras, J. F., E. Santini, and M. Wing, "Calculation of synchronous reactances of small permanent-magnet alternating-current motors: Comparison of analytical approach and finite element method with measurements," *IEEE Trans. on Magnetics*, Vol. 34, No. 5, 3712–3720, Sep. 1998.
6. Rahman, M. A. and P. Zhou, "Determination of saturated parameters of PM motors using loading magnetic fields," *IEEE Trans. on Magnetics*, Vol. 27, No. 5, 3947–3950, Sep. 1991.
7. Nee, H. P., L. Lefevre, P. Thelin, and J. Soulard, "Determination of $d$ and $q$ reactances of permanent-magent synchronous motors without measurements of the rotor position," *IEEE Trans. on Industry Applications*, Vol. 36, No. 5, 1330–1335, Sep.–Oct. 2000.
8. Rahman, K. M. and S. Hiti, "Identification of machine parameters of a synchronous motor," *IEEE Trans. on Industry Applications*, Vol. 41, No. 2, 557–565, Mar.–Apr. 2005.
9. Lee, J. Y., S. H. Lee, G. H. Lee, J. P. Hong, and J. Hur, "Determination of parameters considering magnetic nonlinearity in an interior permanent magnet synchronous motor," *IEEE Trans. on Magnetics*, Vol. 42, No. 4, 1303–1306, Apr. 2006.
10. Hwang, C. C., S. M. Chang, C. T. Pan, and T. Y. Chang, "Estimation of parameters of interior permanent magnet synchronous motors," *Journal of Magnetism and Magnetic Materials*, Vol. 239, 600–603, 2002.
11. Lee, J. Y., J. W. Kim, J. H. Chang, S. U. Chung, D. H. Kang, and

J. P. Hong, "Determination of parameters considering magnetic nonlinearity in solid core transverse flux linear motor for dynamic simulation," *IEEE Trans. on Magnetics*, Vol. 44, No. 6, 1566–1569, Jun. 2008.

12. Qing, A., C. K. Lee, and L. Jen, "Electromagnetic inverse scattering of two-dimensional perfectly conducting objects by real-coded genetic algorithm," *IEEE Trans. Geosci. Remote Sensing*, Vol. 39, No. 3, 665–676, Mar. 2001.
13. Hoole, S. R., S. Subramanian, R. Saldanha, J. L. Coulomb, and J. C. Sabonnadiere, "Inverse problem methodology and finite elements in the identification of cracks, sources, materials, and their geometry in inaccessible locations," *IEEE Trans. on Magnetics*, Vol. 27, No. 3, 3433–3443, May 1991.
14. Favennec, Y., V. Labbé, Y. Tillier, and F. Bay, "Identification of magnetic parameters by inverse analysis coupled with finite element modeling," *IEEE Trans. on Magnetics*, Vol. 38, No. 6, 3607–3619, Nov. 2002.
15. Schreiber, J., J. Haueisen, and J. Nenonen, "A new method for choosing the regularization parameter in time-dependent inverse problems and its applications to magnetocardiography," *IEEE Trans. on Magnetics*, Vol. 40, No. 2, 1104–1107, Mar. 2004.
16. Huang, C. H., J. X. Li, and S. Kim, "An inverse problem in estimating the strength of contaminant source for groundwater systems," *Applied Mathematical Modelling*, Vol. 32, 417–431, 2008.
17. Goharian, M., M. Soleimani, and G. R. Moran, "A trust region subprolem for 3D electrical impedance tomography inverse problem using experimental data," *Progress In Electromagnetics Research*, Vol. 94, 19–32, 2009.
18. Hadamard, J., *Lectures on the Cauchy Problem in Linear Partial Differential Equations*, Yale University Press, New Haven, 1923.
19. Hanke, M., "Limitations of the L-curve method in ill-posed problems," *BIT Numerical Mathematics*, Vol. 36, 287–301, 1996.
20. Gieras, J. F. and M. Wing, *Permanent Magnet Motor Technology: Design and Applications*, Marcel Dekker Inc., New York, 2002.